Interplay between anisotropy and spatial dispersion in metamaterial waveguides

K. L. Koshelev* and A. A. Bogdanov†
ITMO University, 197101 St. Petersburg, Russian Federation
and Ioffe Institute, 194021 St. Petersburg, Russian Federation
(Received 28 April 2016; published 29 September 2016)

We analyze the spectrum of waveguide modes of an arbitrary uniaxial anisotropic metamaterial slab with nonlocal electromagnetic response whose permittivity tensor could be described within the Drude approximation. Spatial dispersion was introduced within the hydrodynamical model. By considering both anisotropy and spatial dispersion as perturbations, we distinguish their effect on the spectrum of the slab and analyze lifting of the degeneracy of eigenmodes at plasma frequency in detail. Spatial dispersion is shown to result in a break of the singularity in the density of optical states in the hyperbolic regime and in suppression of negative dispersion induced by anisotropy. We demonstrate that the interplay of spatial dispersion and anisotropy can bring light to a complete stop at certain frequencies.

DOI: 10.1103/PhysRevB.94.115439

I. INTRODUCTION

The electromagnetic response of metamaterials in the simplest case is described by an effective permittivity and permeability, ε and μ. Spatial inhomogeneity and the retardation effect result in dependence of the effective parameters on the frequency ω and the wave vector $\mathbf{k}$ of the incident wave. Anisotropic, chiral, and bianisotropic metamaterials are described by tensorial effective parameters $\hat{\varepsilon}(\omega,\mathbf{k})$ and $\hat{\mu}(\omega,\mathbf{k})$. The specific form of $\hat{\varepsilon}(\omega,\mathbf{k})$ and $\hat{\mu}(\omega,\mathbf{k})$ depends on the design of metamaterials. However, in the case of the long-wavelength limit ($|\mathbf{k}|L \ll 1$, where L is the characteristic period of the structure), the local electromagnetic response can be often described in the framework of the Drude approach [1–11],

$$\varepsilon(\omega) = \varepsilon_\infty\left[1 - \frac{\Omega^2}{\omega(\omega + i\gamma)}\right]. \tag{1}$$

Here, ε_∞ is the permittivity of a host material, γ is the damping parameter, and Ω is the resonance frequency (plasma frequency) of a metamaterial. In isotropic metamaterials, the resonance frequency Ω is degenerated [4,12]. Structural anisotropy, i.e., the anisotropy of meta-atoms or the lattice of a metamaterial, can lift the degeneracy and dramatically change its properties. For example, the anisotropy of effective masses of charge carriers in conducting layers of periodic metal-dielectric structures results in the appearance of additional allowed energy bands for photons [13]. The hyperbolic regime of metamaterial characterized by a singular density of optical states can be reached for media with anisotropic plasma frequency [7]. The structural anisotropy can be simply tailored at the fabrication stage.

Along with a structural anisotropy, it is possible to distinguish the anisotropy induced by spatial dispersion when an incident electromagnetic wave creates a preferential direction parallel to the wave vector $\mathbf{k}$, which plays the role of an optical axis [14,15]. Usually, in natural media, spatial dispersion is essential only in the vicinity of resonances (interband transitions, exciton absorption, plasmon excitation, etc.) and can be neglected far from them [16,17]. In contrast to that, spatial dispersion in artificial media can be essential even in the long-wavelength limit [18].

In the present paper, we analyze and compare the effects of the spatial dispersion and structural anisotropy on the spectrum of a metamaterial slab. We describe the dielectric function of the slab within the Drude approximation. It is a quite general approach, which is being used for many types of metamaterials from split-ring resonator based structures to wire and multilayer media [4,6,7,9,10,19]. Anisotropy of the slab is introduced through the anisotropy of the plasma frequency. Spatial dispersion is considered within the hydrodynamical approximation. In order to distinguish the effects of spatial dispersion and structural anisotropy, we consider them as perturbations [20]. In contrast to the previous works related to the nonlocal response of metamaterials, we focus on the interplay between the anisotropy and the spatial dispersion [21–25]. Particularly, we show that such interplay can lead light to a complete stop at certain frequencies.

The paper is organized as follows. In Sec. II A, we briefly discuss the spectrum of a bulk isotropic metamaterial. In Secs. II B and II C, we consistently analyze spectra of isotropic and anisotropic metamaterial slabs, neglecting any spatial dispersion effects. In Secs. II D and II E, we study the effects of nonlocal electromagnetic response on the waveguide spectra of isotropic and anisotropic metamaterial slabs, respectively. In Sec. III, we analyze the case of a finite dielectric contrast between the cladding layers and the slab. In Sec. IV, we discuss the figure of merit and dissipation spectra. Finally, in Sec. V, we summarize our major results.

II. GUIDED MODES DISPERSION

A. Bulk metamaterial

Before turning to the problem of a metamaterial slab, let us briefly consider the eigenmode spectrum of a bulk isotropic metamaterial with an arbitrary scalar permittivity $\varepsilon(\omega,\mathbf{k})$.

Spatial and time Fourier transform of Maxwell's equation $\nabla \cdot \mathbf{D} = 0$ in the isotropic case yields

$$\varepsilon(\omega,\mathbf{k})[\mathbf{k} \cdot \mathbf{E}(\omega,\mathbf{k})] = 0. \tag{2}$$

*ki.koshelev@gmail.com
†bogdanov@ioffe.mail.ru

Equation (2) has two solutions: (i) transversal electromagnetic waves satisfying the condition $\mathbf{E}\perp\mathbf{k}$ and (ii) longitudinal waves satisfying the equation $\varepsilon(\omega,\mathbf{k})=0$ [26]. The longitudinal waves are pure electric ($\mathbf{H}=0$) [14]. In plasma, metal or semiconductor, they represent oscillations of charge carrier density and are often called bulk plasma waves or Langmuir waves [27,28]. In a medium with local electromagnetic response, the frequency of Langmuir waves does not depend on both the direction and absolute value of the wave vector $\mathbf{k}$. Thus, Langmuir waves form an infinite set of degenerated modes with zero group velocity.

Spatial dispersion results in a dependence of the frequency of the longitudinal wave on the absolute value of $\mathbf{k}$, but not on its direction. So, the degeneracy is lifted only partially. Total lift of the degeneracy demands the existence of an additional preferential direction not parallel to $\mathbf{k}$. In a bulk medium, it can be induced, for example, by an external magnetic field or by anisotropy of the effective mass of carriers [8,29]. In the case of a slab, the preferential direction is naturally determined by the normal to the slab's interfaces.

B. Isotropic slab

Let us consider a metamaterial slab (with thickness a) with local isotropic electromagnetic response described in the framework of the Drude approach [see Eq. (1)]. The spectrum of such a slab consists of three types of eigenmodes: (i) bulk waveguide modes formed due to total reflection of electromagnetic waves from the slab boundaries, (ii) two surface modes formed due to constructive and destructive interference of the surface waves localized at the slab's boundaries, and (iii) Langmuir modes formed due to reflection of pure electric longitudinal waves from the slab's boundaries. The properties of the bulk and surface modes are well documented (see, e.g., Refs. [30–34]), so we mainly focus on the properties of the Langmuir ones. The latter are TM polarized only and, therefore, have two components of electric field satisfying the equation

$$E_x=-\frac{i}{k_z}\frac{\partial E_z}{\partial x}. \tag{3}$$

Here, k_z is the lateral component of the wave vector. As in infinite metamaterial, the Langmuir modes do not satisfy the Helmholtz equation, being at the same time a solution of the Maxwell's equation $\mathrm{div}\mathbf{D}=0$. Straightforward analysis of the Maxwell's equations and matching conditions at the boundaries shows that the electric field of the Langmuir modes is completely confined in the slab and does not penetrate into the cladding layers independently of their permittivity. The frequency of the Langmuir modes does not depend on k_z and coincides with plasma frequency of the slab Ω as in a bulk metamaterial. Therefore, in an isotropic metamaterial slab, Langmuir waves represent a degenerated set of eigenmodes with zero group velocity. Introducing the losses ($\gamma\neq 0$) into the slab does lift the degeneracy, making the frequency a complex value $\omega\approx\Omega-i\gamma/2$.

An example of the mode structure of an isotropic metamaterial slab is shown in Fig. 2(a). For the sake of simplicity, the cladding layers are assumed to be perfectly conducting

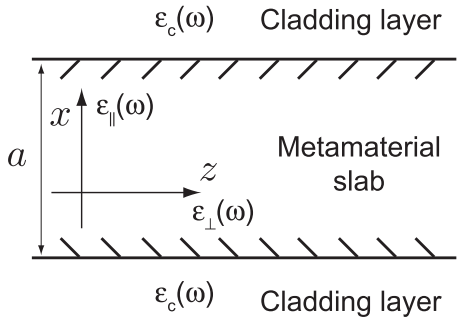

FIG. 1. Metamaterial slab with plasma core and arbitrary cladding layers. Guided modes propagate along the z axis.

[31,35]. The case of a finite dielectric contrast between the cladding layers and the slab is considered further in Sec. II E.

C. Anisotropic slab

Let us consider a metamaterial slab with uniaxial anisotropic permittivity with the optical axis parallel to the x direction (see Fig. 1). The permittivity tensor in this case is given by

$$\hat{\varepsilon}_s(\omega)=\begin{pmatrix}\varepsilon_\parallel(\omega) & 0 & 0\\ 0 & \varepsilon_\perp(\omega) & 0\\ 0 & 0 & \varepsilon_\perp(\omega)\end{pmatrix}. \tag{4}$$

Here, indices $\parallel$ and $\perp$ correspond to directions along and across the optical axis. We suppose that the tensor components have Drude dispersion [see Eq. (1)] with different plasma frequencies $\Omega_\perp$ and $\Omega_\parallel$. Parameter ε_∞ is supposed to be isotropic.

The Helmholtz equation for the TM-polarized modes inside the slab is reduced to the following:

$$\varepsilon_\parallel\frac{\partial^2 E_x}{\partial x^2}+\varepsilon_\perp\left(\varepsilon_\parallel\frac{\omega^2}{c^2}-k_z^2\right)E_x=0. \tag{5}$$

Analytical expression for the dispersion of the Langmuir and bulk waveguide modes can be straightforwardly obtained from Eq. (5) in the case of a perfect electric conductor boundary condition,

$$k_z^2=\varepsilon_\parallel\left(\frac{\omega^2}{c^2}-\frac{\pi^2 n^2}{a^2\varepsilon_\perp}\right). \tag{6}$$

Here, $n=0,1,2,\ldots$ is an integer mode number. Figure 2(b) shows the dispersion of Langmuir and bulk waveguide modes for the case $\Omega_\perp>\Omega_\parallel$. One can see that the degeneracy for the Langmuir modes is lifted. Their spectrum is sandwiched between plasma frequencies $\Omega_\perp$ and $\Omega_\parallel$, where $\varepsilon_\parallel\varepsilon_\perp<0$ and the metamaterial slab exhibits the properties of a hyperbolic medium [36,37]. The density of states for the Langmuir modes is singular for any frequency $\Omega_\parallel<\omega<\Omega_\perp$ as all of the modes [except one corresponding to $\varepsilon_\perp(\omega)=0$] have the common frequency cutoff $\Omega_\parallel$ and the common horizontal asymptote $\omega=\Omega_\perp$. Only the fundamental Langmuir mode ($n=0$) is pure electrical. The rest of the Langmuir modes have nonzero magnetic field and, therefore, nonzero Poynting vector. Their group velocity $\mathbf{v}_g=\partial\omega/\partial k_z$ can be found from Eq. (6). In the

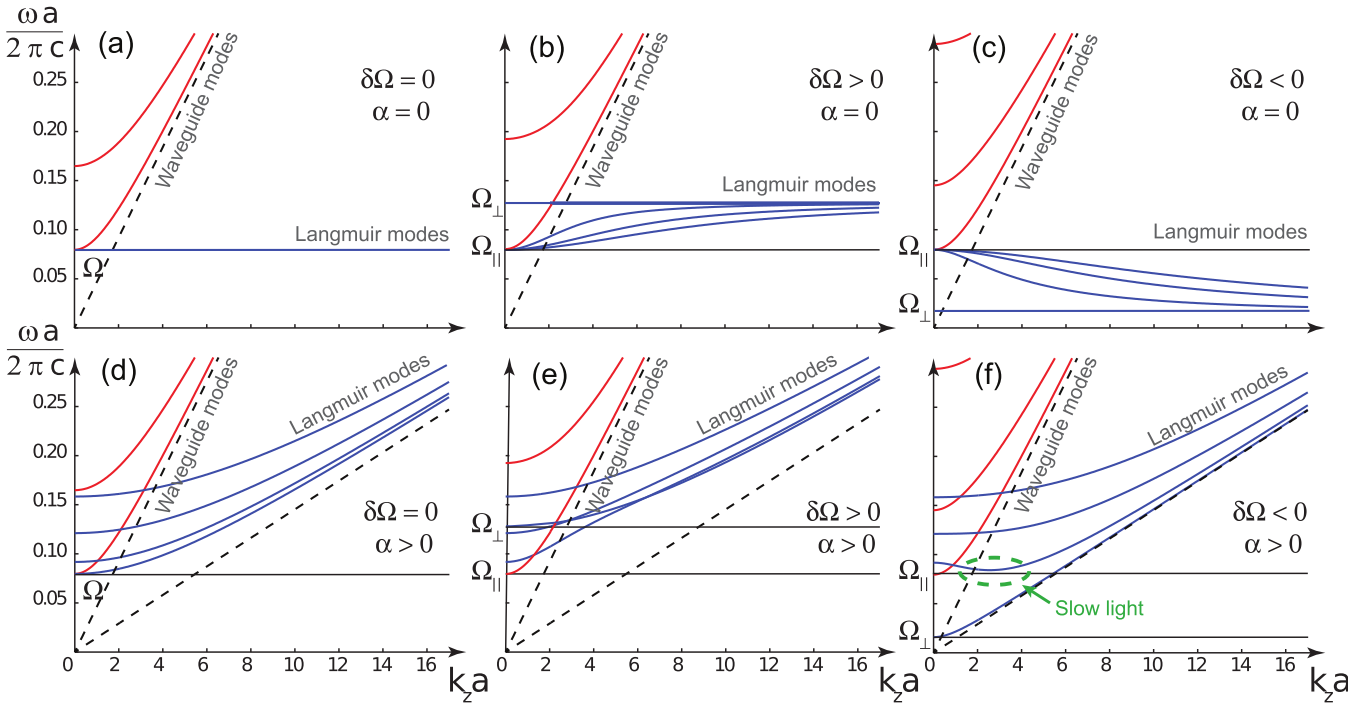

FIG. 2. Dispersion of TM-polarized guided modes propagating inside the metamaterial slab with metal claddings. Red solid lines show the dispersion of fast conventional waveguide modes; blue solid lines picture the dispersion of slow Langmuir modes. Black dashed lines represent the light lines $\omega = ck_z/\sqrt{\varepsilon_\infty}$ and $\omega = Cvk_z/\sqrt{\varepsilon_\infty}$, which describe the asymptotical behavior of fast and slow modes correspondingly. Black horizontal solid lines show plasma frequencies $\Omega_\parallel a/2\pi c$ and $\Omega_\perp a/2\pi c$. The insets describe the regime, i.e., the magnitude of anisotropy ($\delta\Omega$) and nonlocal effects (α). The parameters are $\alpha = 0.1$, $\varepsilon_\infty = 12$.

case of $\Omega_\parallel > \Omega_\perp$, the dispersion of the Langmuir modes is negative [see Fig. 2(c)].

In spite of the existence of the analytical expression for the dispersion [see Eq. (6)], a simpler way to analyze the spectrum of the Langmuir modes and to gain deep insight into how the anisotropy lifts the degeneracy is to consider the anisotropy as a perturbation. Let us take the difference between plasma frequencies along the $\parallel$ and $\perp$ directions as a perturbation parameter ($\delta\Omega = \Omega_\perp - \Omega_\parallel$) assuming that $|\delta\Omega| \ll \Omega_\parallel, \Omega_\perp$.

Using the perturbation theory for the case of a degenerate spectrum, one can find the set of zeroth-order eigenfunctions whose modification under the action of the small applied perturbation is small,

$$E_z = E_0 \sin\left(\frac{\pi n x}{a}\right), \quad E_x = -E_0 \frac{i\pi n}{ak_z} \cos\left(\frac{\pi n x}{a}\right). \tag{7}$$

Here, $n = 0,1,2,\ldots$ is the mode number as in Eq. (6). It follows from Eq. (7) that the Langmuir modes are nearly longitudinal if $n \ll k_z a$ and nearly transversal if $n \gg k_z a$.

Perturbation to the eigenfrequency of Langmuir mode $\delta\omega_n$ is readily found as

$$\delta\omega_n = \delta\Omega \frac{k_z^2}{k_z^2 + \left(\frac{\pi n}{a}\right)^2}. \tag{8}$$

On can see that perturbation theory works for all mode numbers n for both short- and long-wavelength limits as $|\delta\omega_n| \leqslant |\delta\Omega|$ for all k_z. Equation (8) also predicts the right sign of group velocity for the Langmuir modes.

As was mentioned earlier, in the case of an anisotropic slab, the Langmuir modes are not pure electric waves. Their magnetic field is given by

$$H_y = -2i\delta\Omega\varepsilon_\infty E_0 \frac{\left(\frac{\pi n}{a}\right)}{c\left[k_z^2 + \left(\frac{\pi n}{a}\right)^2\right]} \cos\left(\frac{\pi n x}{a}\right). \tag{9}$$

One can see that the magnetic field does not vanish at the slab's boundaries and, therefore, penetrates inside the cladding layers.

D. Isotropic slab with effects of nonlocality

The problem of spatial dispersion has a long history and is still being discussed [16,18,38–46]. The main stumbling block of the spatial dispersion problem is the additional boundary condition (ABC). Indeed, the presence of an additional wave due to nonlocal response requires an ABC to determine the amplitude of the longitudinal wave. We will discuss the appropriate choice of the ABC below.

In the presence of a weak nonlocality, electric induction $\mathbf{D}$ can be expressed through electric field $\mathbf{E}$ as (see, e.g., Ref. [40])

$$\mathbf{D} = \varepsilon_s(\omega)\mathbf{E} + C_1 \mathrm{grad}(\mathrm{div}\mathbf{E}) + C_2 \mathrm{rot}(\mathrm{rot}\mathbf{E}). \tag{10}$$

The second term affects only the transversal waves, while the first one affects only the longitudinal waves. The coefficients C_1 and C_2 can have a frequency dependence, which is determined by the particular physical model. We will analyze the spatial dispersion within the hydrodynamical approximation which takes into account only the first two terms of Eq. (10).

This approximation is often used for the description of plasma oscillations in condensed-matter systems including wire media and nanoparticle composites [47–52]. It describes the motion of the charges by the Euler equation that results in the following dependence of $\mathbf{D}$ on $\mathbf{E}$:

$$\mathbf{D} = \hat{\varepsilon}_s \mathbf{E} + C\frac{v^2}{\omega(\omega + i\gamma)}\mathrm{grad}(\mathrm{div}\mathbf{E}). \tag{11}$$

Here, C is a numerical constant and v is the mean velocity of the chaotic motion of charges. In the case of nondegenerate plasma, v represents the thermal velocity of carriers and $C = 1/3$ [44]. In the case of degenerate plasma, v is the Fermi velocity and $C = 3/5$ [44]. For now, we put $\gamma = 0$. The effect of losses will be considered further in Sec. IV.

Let us note that as follows from Eq. (11), the nonlocal response is of the order of $(vk/\omega)^2$. Therefore, it is significant only for the modes with low phase velocity ω/k comparable with characteristic velocity of carriers v, i.e., only for the Langmuir and surface modes.

Substitution of electrical displacement $\mathbf{D}$ from Eq. (11) into the Maxwell's equations yields the Helmholtz equation of the fourth order for TM-polarized waves,

$$\left[\alpha\frac{\partial^2}{\partial x^2} + \alpha\left(k_x^{\mathrm{s}}\right)^2\right]\left[\frac{\partial^2}{\partial x^2} + \left(k_x^{\mathrm{f}}\right)^2\right]E_x = 0, \tag{12}$$

$$\left(k_x^{\mathrm{s}}\right)^2 = \frac{\varepsilon_s\omega^2}{\alpha c^2} - k_z^2, \tag{13}$$

$$\left(k_x^{\mathrm{f}}\right)^2 = \frac{\varepsilon_s\omega^2}{c^2} - k_z^2. \tag{14}$$

The wave-vector components k_x^{f} and k_x^{s} correspond to the fast (waveguide) and slow (Langmuir) modes, respectively. The parameter $\alpha = Cv^2/c^2$ is the dimensionless quantity characterizing the spatial dispersion.

By virtue of symmetry, the general solution inside the slab can be divided into symmetric and antisymmetric:

$$E_x(x) = A\begin{Bmatrix}\cos\left(k_x^{\mathrm{f}}x\right)\\ \sin\left(k_x^{\mathrm{f}}x\right)\end{Bmatrix} + B\begin{Bmatrix}\cos\left(k_x^{\mathrm{s}}x\right)\\ \sin\left(k_x^{\mathrm{s}}x\right)\end{Bmatrix}. \tag{15}$$

The magnetic field is nonzero only for the fast modes,

$$H_y(x) = A\frac{\varepsilon_s\omega}{ck_z}\begin{Bmatrix}\cos\left(k_x^{\mathrm{f}}x\right)\\ \sin\left(k_x^{\mathrm{f}}x\right)\end{Bmatrix}. \tag{16}$$

In the general case, eigenmodes represent a superposition of fast and slow modes. The ratio between the amplitudes A and B is determined from the ABC. The ABC depend on the model used to describe the spatial dispersion and, generally speaking, they should be determined microscopically [42,53]. Correct ABC is not a matter of choice, but can be derived from the nonlocal hydrodynamic equations, at least for a given equilibrium free-electron density profile. In the case of dielectric claddings, we assume that the equilibrium free-electron density of the core has a step profile, i.e., it is constant inside the core and abruptly drops to zero at the boundary [44,52,54]. Under this assumption, the continuity equation readily gives the ABC,

$$\mathbf{J}\cdot\hat{\mathbf{n}} = 0, \tag{17}$$

stating that the normal component of the induced current density $\mathbf{J}$ vanishes at the boundary. In terms of normal components of electric fields, Eq. (17) can be rewritten as

$$\varepsilon_\infty E_x^{\mathrm{s}} = \varepsilon_{\mathrm{c}} E_x^{\mathrm{c}}, \tag{18}$$

where $E_x^{\mathrm{s}}, E_x^{\mathrm{c}}$ are the field components inside the slab and the claddings, respectively, and ε_{c} is the permittivity of the cladding layers.

However, if the penetration of the modes into the cladding layers is weak or the claddings are made of perfect electric conductor, we can use a rough model and neglect the interaction between the fast and the slow modes. Therefore, the wave vectors k_x^{f} and k_x^{s} can be quantized independently as $\pi n/a$. Dispersions of the waveguide and Langmuir modes are given by

$$\left(\omega_n^{\mathrm{f}}\right)^2 = \Omega^2 + \frac{c^2}{\varepsilon_\infty}\left[k_z^2 + \left(\frac{\pi n}{a}\right)^2\right], \tag{19}$$

$$\left(\omega_n^{\mathrm{s}}\right)^2 = \Omega^2 + \frac{\alpha c^2}{\varepsilon_\infty}\left[k_z^2 + \left(\frac{\pi n}{a}\right)^2\right]. \tag{20}$$

Their plot is shown in Fig. 2(d) by red and blue lines, respectively.

One can see that the degeneracy of Langmuir modes is lifted. Moreover, spatial dispersion results in dependence of their cutoff frequencies on the mode number n. Therefore, the singularity in the density of optical states is destroyed because there is only a finite number of the modes at any fixed frequency ω.

Let us note that the Poynting vector $\mathbf{S}$ defined as $\frac{c}{8\pi}\mathrm{Re}[\mathbf{E}\times\mathbf{H}]$ is zero for the Langmuir modes as they are pure electric modes. However, their group velocity is nonzero. There is no contradiction because the Langmuir modes transfer the energy accumulated by electron gas due to its compression and expansion, while fast waveguide modes transfer energy due to nonzero electric and magnetic fields [43]. Therefore, we have different mechanisms of the energy transfer for the Langmuir and waveguide modes.

As mentioned above, we neglect the interaction between the Langmuir and waveguide modes and, therefore, avoid consideration of ABCs. Accounting for an interaction between the Langmuir and waveguide modes results in the appearance of anticrossing between their dispersion curves [55,56]. In a symmetric waveguide, the interaction is possible only between modes of the same parity. The strength of the splitting depends on the ABCs and is calculated for the case of dielectric claddings below.

E. Anisotropic slab with effects of nonlocality

Now let us take into account both anisotropy of the slab and nonlocality within the hydrodynamical approach. The Helmholtz equation for the TM-polarized wave in this case can be obtained straightforwardly from the Maxwell's

equations:

$$\alpha\frac{\partial^2}{\partial x^2}\left[\frac{\partial^2 E_x}{\partial x^2}+\left(\frac{\varepsilon_\perp\omega^2}{c^2}-k_z^2\right)E_x\right]+\left(\frac{\varepsilon_\parallel\omega^2}{c^2}-\alpha k_z^2\right)\frac{\partial^2 E_x}{\partial x^2}$$
$$+\left(\frac{\varepsilon_\perp\omega^2}{c^2}-\alpha k_z^2\right)\left(\frac{\varepsilon_\parallel\omega^2}{c^2}-k_z^2\right)E_x=0. \quad (21)$$

Equation (21) can be written in the compact form using the substitution $E_x\propto e^{\pm ik_x x}$,

$$\frac{\omega^2}{(1-\alpha)c^2}=\frac{k_x^2}{\varepsilon_\perp(\omega,k)}+\frac{k_z^2}{\varepsilon_\parallel(\omega,k)}. \quad (22)$$

Here, we use the following notations:

$$\varepsilon_{\perp,\parallel}(\omega,k)=\varepsilon_{\perp,\parallel}(\omega)-\alpha\frac{c^2\left(k_x^2+k_z^2\right)}{\omega^2}. \quad (23)$$

Equation (22) is biquadratic. Its solutions $\pm k_x^{\mathrm{f}}$ and $\pm k_x^{\mathrm{s}}$ correspond to the slow and the fast modes with symmetric and antisymmetric field distribution. Dispersion of the eigenmodes depends on the boundary conditions which define the quantization rule for k_x^{f} and k_x^{s}. As in the previous section, we will quantize k_x^{f} and k_x^{s} independently as $\pi n/a$ assuming that the interaction between slow and fast modes is vanishingly small and penetration depth of the modes in the slab claddings is negligible. The dispersions $\omega_n^{\mathrm{f,s}}(k_z)$ found from Eq. (22) for the cases $\Omega_\parallel<\Omega_\perp$ and $\Omega_\parallel>\Omega_\perp$ are shown in Figs. 2(e) and 2(f), respectively. The analytical expressions for $\omega_n^{\mathrm{f,s}}$ are cumbersome and not convenient for analysis. The compact expressions can be obtained within perturbation theory assuming that $|\delta\Omega|\ll\Omega_{\parallel,\perp}$ and $v\ll c$, and reveal particular contributions of anisotropy and nonlocal effects:

$$\left(\omega_n^{\mathrm{f}}\right)^2=\Omega^2\left[1+\frac{2\delta\Omega}{\Omega}\frac{\frac{\pi^2n^2}{a^2}}{\frac{\pi^2n^2}{a^2}+k_z^2}\right]+\frac{c^2}{\varepsilon_\infty}\left[k_z^2+\frac{\pi^2n^2}{a^2}\right], \quad (24)$$

$$\left(\omega_n^{\mathrm{s}}\right)^2=\Omega^2\left[1+\frac{2\delta\Omega}{\Omega}\frac{k_z^2}{\frac{\pi^2n^2}{a^2}+k_z^2}\right]+\frac{\alpha c^2}{\varepsilon_\infty}\left[k_z^2+\frac{\pi^2n^2}{a^2}\right]. \quad (25)$$

One can see that in contrast to anisotropy, spatial dispersion affects only the Langmuir modes. Simple analysis of Eq. (25) yields that Langmuir modes exhibit negative dispersion if $\delta\Omega<0$ for $k_z<k_z^*$, where

$$k_z^*=\frac{\pi n}{a}\left(\frac{n^*}{n}-1\right)^{1/2}. \quad (26)$$

Here, n^* is the maximal index of the Langmuir mode for which negative dispersion exists,

$$n^*=\frac{a}{\pi}\sqrt{\frac{2\Omega|\delta\Omega|\varepsilon_\infty}{\alpha c^2}}. \quad (27)$$

Spatial dispersion and anisotropy contribute counteractingly into the energy flow for the Langmuir modes. Therefore, the flows of electromagnetic and mechanic energy can completely compensate each other and bring the Langmuir mode to a complete stop. Slow light can be observed at the frequency $\omega_n^{\mathrm{s}}(k_z^*)$. This allows one to reach the cavity regime without mirrors similarly to distributed feedback cavities [57,58].

It should be mentioned that anisotropy does not affect the fundamental Langmuir mode ($n=0$), so it remains pure electric ($H_y=0$) and longitudinal ($E_x=0$). Dispersion of the main Langmuir mode is determined by equation $\varepsilon_\perp(\omega,k_z)=0$. Therefore, it is always positive. For other Langmuir modes, the frequency bandwidth $\Delta\omega$ of negative dispersion depends on the mode number n as

$$\Delta\omega=\omega_n^{\mathrm{s}}(0)-\omega_n^{\mathrm{s}}(k_z^*)\approx|\delta\Omega|\left(\frac{n}{n^*}-1\right)^2. \quad (28)$$

III. EFFECT OF CLADDING LAYERS

In the previous sections, we neglected the penetration depth of the field inside the cladding layers assuming that the dielectric contrast between them and the metamaterial slab is infinitely high. Within this assumption, k_x^{f} and k_x^{s} can be quantized independently as $\pi n/a$. Here, we analyze the effect of the finite dielectric contrast on the dispersion of the eigenmodes.

A finite dielectric contrast results in the appearance of two surface waves in the spectrum forming due to constructive and destructive interference of surface plasmon-polariton (SPP) modes localized at the slab interfaces. The electromagnetic properties of SPPs are well documented and we do not focus on them [8,32–34,59–61].

Penetration of the modes inside the cladding layers effectively changes the thickness of the slab. The correction to k_x^{f} in the isotropic case within the assumption of high dielectric contrast ($|\varepsilon_{\mathrm{s}}/\varepsilon_{\mathrm{c}}|\gg1$) can be derived from the expression for the Goos-Hanchen shift [62–67]:

$$\delta k_{x,n}^{\mathrm{f}}=-\frac{\varepsilon_{\mathrm{c}}\varepsilon_{\mathrm{s}}\omega^2/c^2}{\sqrt{k_z^2-\varepsilon_{\mathrm{c}}\omega^2/c^2}}\frac{2\pi n}{\varepsilon_{\mathrm{s}}(\omega)k_z^2a^2-\varepsilon_{\mathrm{c}}\pi^2n^2}. \quad (29)$$

Here, ε_{c} is the permittivity of the cladding layers. One can see that in the case of metal cladding layers $\varepsilon_{\mathrm{c}}<0$, the correction is purely real and positive which corresponds to a negative Goos-Haanchen shift. However, in the case of dielectric cladding layers, $\varepsilon_{\mathrm{c}}>0$, the correction is real under light line $\varepsilon_{\mathrm{c}}^{1/2}\omega/c=k_z$ and imaginary above the light line where the modes are leaky.

It should be mentioned that in the isotropic case and when we neglect the mixing between the Langmuir and waveguide modes, the cladding layers do not affect the dispersion of the Langmuir modes at all since they are perfectly confined inside the slab. Therefore, in the framework of this approach, the Langmuir modes remain nonleaky above the light line of the cladding layers, in sharp contrast to the waveguide modes. However, a deeper analysis shows that the Langmuir modes penetrate into the cladding layers and have leakage losses above the light line. It occurs because of their mixing with waveguide modes which is determined by the ABC [see Eq. (18)]. Detailed analysis of the interaction between Langmuir and waveguide modes and their coupling in the presence of an appropriate ABC is presented in the Supplemental Material [56].

It is important to note that the physics underlying our method of stopping the light qualitatively differs from the

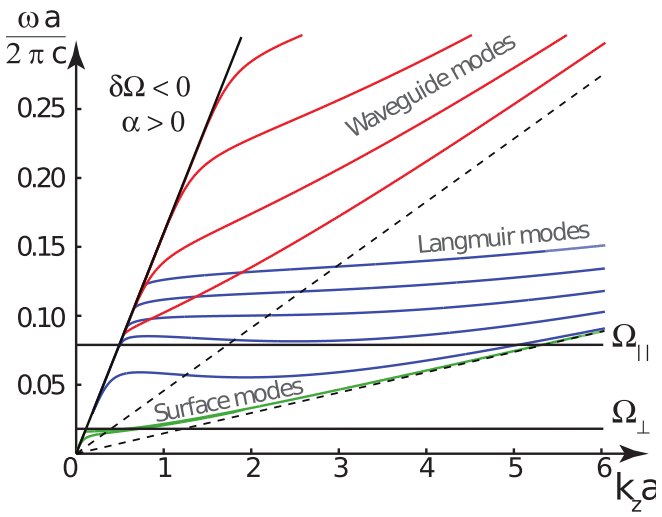

FIG. 3. Dispersion of TM-polarized guided modes propagating inside the metamaterial slab with dielectric claddings with constant permittivity ε_c. Red solid lines show the dispersion of fast conventional waveguide modes, blue solid lines picture the dispersion of slow Langmuir modes, and green solid lines show the dispersion of slow surface plasmon-polariton modes. Black horizontal solid lines show plasma frequencies $\Omega_\parallel a/2\pi c$ and $\Omega_\perp a/2\pi c$. Black dashed lines represent the light lines $\omega = ck_z/\sqrt{\varepsilon_\infty}$ and $\omega = Cvk_z/\sqrt{\varepsilon_\infty}$, which describe the asymptotical behavior of fast and slow modes correspondingly. The black inclined solid line represents the light line $\omega = ck_z/\sqrt{\varepsilon_c}$, which separates the region of leaky and stable modes. The parameters are $\alpha = 0.1$, $\varepsilon_\infty = 12$, $\varepsilon_c = 1$.

well-known approach used in planar waveguides. Usually, one considers a metal slab with dielectric claddings (or a dielectric slab with metal claddings) where the Goos-Haanchen shift is negative because of different direction of energy flow in the claddings and the core. For certain waveguide parameters, the positive and the negative flows can cancel each other, forming a closed-loop energy vortex associated with zero group velocity [67]. Quite contrary, in our approach, the slow light regime exists even for a waveguide with claddings made of perfect electric conductor. It happens because we reach the cancellation of mechanical and electromagnetic energy flows, which both exist inside the core layer.

The dispersion $\omega(k_z)$ of TM-polarized modes inside the anisotropic plasma slab with dielectric claddings ($\varepsilon_c > 0$) in the presence of spatial dispersion is shown in Fig. 3. Parameters of the structure are described in the caption of the figure. Fast, slow, and surface modes are shown with red, blue, and green lines, respectively.

IV. LOSSES

Dissipation spectra of the waveguide and surface modes are well documented (see, e.g., Refs. [68–70]), so here we focus on the Langmuir modes only. We include loss in our model by setting the damping rate γ in Eq. (1) to a finite nonzero value. In general, lossy structures support two sets of solutions, namely, complex–wave-vector modes and an alternative set of complex-frequency modes [71]. The latter are shown to retain the point of zero group velocity even in the presence of losses [72]. We will discuss this interesting phenomenon further. Within this section, we calculate the figure of merit and show how the spectrum of Langmuir modes modifies in the presence of finite γ. A detailed description of the numerical method used to calculate the modal characteristics is presented in the Supplemental Material [56].

We consider the case of an anisotropic metamaterial slab with a nonlocal electromagnetic response. For the sake of simplicity, we assume that the claddings are made of a perfect electric conductor and that the waveguide and Langmuir modes are not coupled. First, we study the set of modes with real frequency ω and complex longitudinal propagation constant k_z. This approach describes the attenuation of the wave packet with its passage through the material. In this case, the figure of merit (FOM) can be introduced as

$$\eta(\omega) = \frac{\mathrm{Re}(k_z)}{\mathrm{Im}(k_z)}. \tag{30}$$

The meaning of such defined $\eta(\omega)$ is the free path measured in wavelength units. The analytical expression for $\eta(\omega)$ of the Langmuir modes in the hyperbolic regime neglecting the spatial dispersion can be carried out straightforwardly from Eqs. (22) and (23),

$$\eta(\omega) = \frac{2}{\gamma\omega}\left|\frac{(\omega^2-\Omega_\perp^2)(\omega^2-\Omega_\parallel^2)}{\Omega_\parallel^2-\Omega_\perp^2}\right|. \tag{31}$$

One can see that the FOM reaches the maximum value

$$\eta_{\max} = \frac{|\Omega_\perp - \Omega_\parallel|}{\gamma} \quad \text{at} \quad \omega^* = \sqrt{\frac{\Omega_\parallel^2+\Omega_\perp^2}{2}}. \tag{32}$$

The comparison of $\eta(\omega)$ with the results of the numerical simulations [Figs. 4(a) and 4(b)] shows that Eq. (31) works well for high mode numbers ($n \gg 1$).

Propagation of the Langmuir modes at high frequencies ($\omega > \Omega_{\perp,\parallel}$) is possible only in a spatially dispersive media. In this case, the anisotropy is not essential ($\varepsilon_\perp \approx \varepsilon_\parallel$) and the FOM can be estimated from Eqs. (22) and (23) as

$$\eta(\omega) = \frac{2}{\gamma\omega}(\omega^2-\Omega_\perp^2). \tag{33}$$

The comparison of this expression with the results of numerical simulations [Figs. 4(a) and 4(b)] shows that it works well for low mode numbers n.

Modal characteristics of complex-k solutions with quantization number $n = 1$ are shown in Fig. 4(c) for the case of low losses and in Fig. 4(d) for the case of high losses. Real parts $\omega[\mathrm{Re}(k_z)]$ and imaginary parts $\omega[\mathrm{Im}(k_z)]$ are shown with solid and dashed lines, respectively. One can see that a backbending occurs in the modal dispersion curve around the point where the group velocity would have been zero in a loss-free waveguide. Indeed, the propagation loss (which is inverse to the propagation length) would tend to infinity at the stopping point. Thus, the dissipative losses prevent the stopping of complex-k waves in realistic waveguides [73]. The increase of losses [see the transition from Fig. 4(c) to Fig. 4(d)] results in dramatic increase of $\mathrm{Im}(k_z)$. It follows that the modal decay length is shorter than the wavelength in the propagation direction and the concept of group velocity is no longer a good measure of propagation in this region of the dispersion curve.

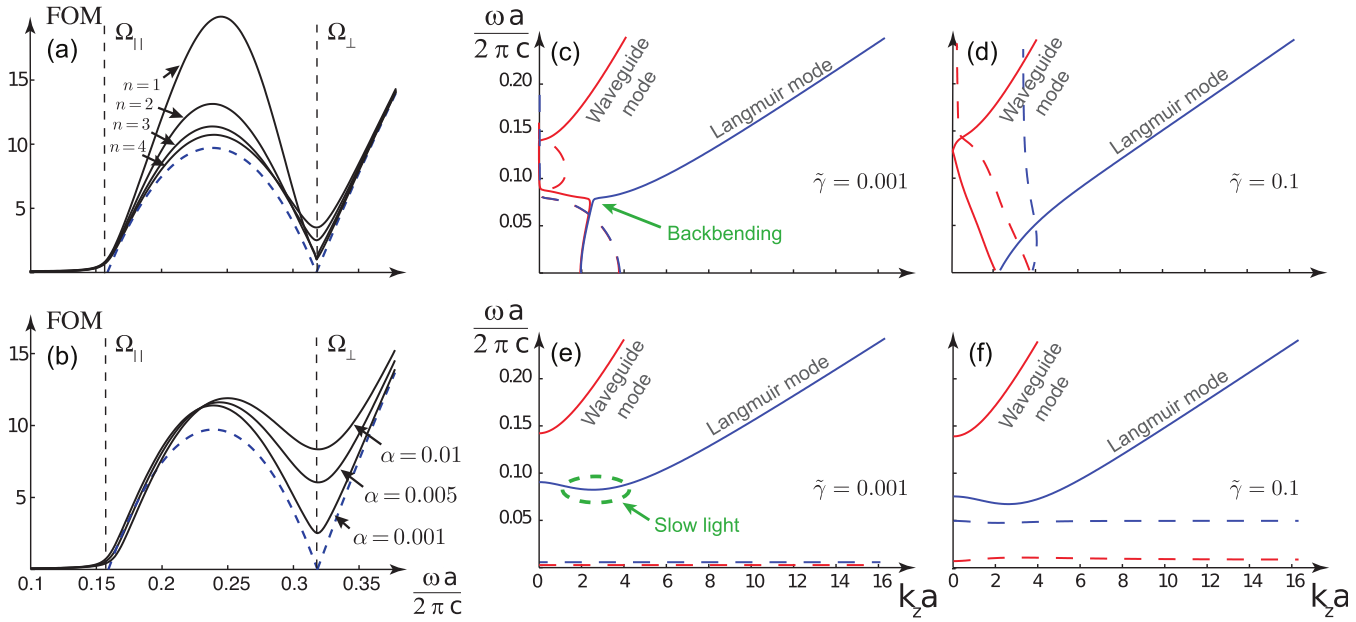

FIG. 4. Effects of losses in the anisotropic metamaterial slab with nonlocal electromagnetic response and with the claddings made of perfect electric conductor. (a),(b) Dependence of complex-k figure of merit η on the frequency ω. Black solid lines represent numerical calculations. Blue dashed lines represent data from analytical expressions (31) and (33). The parameters are $\gamma a/2\pi c = 0.1$, $\varepsilon_\infty = 12$. (a) Dependence of η on ω for different mode numbers n. Parameter α is assumed to be equal to 0.001. (b) Dependence of η on ω for different α. Mode number n is assumed to be equal to 3. (c)–(f) Dispersion diagram of the $n = 1$ (c),(d) complex-k and (e),(f) complex-ω modes. Solid lines represent real parts, while the dashed lines show the corresponding imaginary parts of dispersion, i.e., (c),(d) $\omega[\mathrm{Im}(k_z)]$ and (e),(f) $\mathrm{Im}[\omega(k_z)]$. The parameters are $\alpha = 0.1$, $\Omega_{\|}a/2\pi c = 0.08$, $\Omega_{\perp}a/2\pi c = 0.01$, $\varepsilon_\infty = 12$. Here, $\tilde{\gamma} = \gamma a/2\pi c$ is the dimensionless damping parameter. The complex-ω state retains the zero-group-velocity point independently of γ.

Also the definition of FOM [see Eq. (30)] becomes ill defined because of essential smearing of the wave package.

Next, we switch to another set of solutions with real k_z and complex ω. Such a description is suitable for modes that do not spatially decay, but change uniformly in space as a function of time. In this case, the figure of merit could be redefined as

$$\eta(k_z) = \frac{\mathrm{Re}(\omega)}{\mathrm{Im}(\omega)}. \tag{34}$$

The spectrum of real $\mathrm{Re}[\omega(k_z)]$ and imaginary $\mathrm{Im}[\omega(k_z)]$ parts of complex-ω solutions is shown in Fig. 4(e) for the case of low losses and in Fig. 4(f) for high losses. As above, real and imaginary parts are shown with solid and dashed lines, respectively. Importantly, dispersion curves in the slow light regime do not exhibit backbending when loss is present, thus retaining points where the group velocity goes to zero [72]. This is explained by the fact that since the loss is defined purely in time, it has no dependence on the propagation speed and remains finite at the stopped light point. However, the possibility of complete stop of light for realistic lossy materials is still being discussed [74,75]. One can also note that dispersion curves are barely changed when loss is increased [see the transition from Fig. 4(e) to Fig. 4(f)].

V. SUMMARY

In this paper, we developed the theory of an anisotropic metamaterial waveguide with nonlocal electromagnetic response. Anisotropy and spatial dispersion were taken into account as perturbation that allows one to distinguish their effect on the waveguide spectrum.

It was shown that the anisotropy of plasma oscillations lifts the degeneracy of the Langmuir modes, while keeping their density of states singular. On the contrary, even small spatial dispersion destroys the singularity.

Spatial dispersion and anisotropy can make oppositely directed contributions into the energy flow for the Langmuir modes. Such interplay can bring light to a complete stop. This allows one to reach the cavity regime without any mirrors, similar to distributed feedback cavities.

We have shown that the Langmuir modes in an isotropic waveguide are perfectly confined even above the light line of the cladding layers. They may become leaky either because of anisotropy of the waveguide or because of the resonance mixing with leaky modes, which occurs due to the spatial dispersion effects.

ACKNOWLEDGMENTS

The authors are grateful to I. S. Sinev for useful discussions and proofreading. The theoretical approaches have been developed with a partial support of RFBR (Grants No. 14-02-01223, No. 16-37-60064, No. 15-32-20665), the President of Russian Federation (Grant No. MK- 6462.2016.2), and FASIE. Numerical simulations have been supported by the Russian Science Foundation (Grant No. 15-12-20028).

[1] J. Brown, in *Proceedings of the IEE-Part IV: Institution Monographs* (IEE, London, 1953), Vol. 100, pp. 51–62.

[2] J. B. Pendry, A. J. Holden, W. J. Stewart, and I. Youngs, Phys. Rev. Lett. **76**, 4773 (1996).

[3] A. L. Pokrovsky and A. L. Efros, Phys. Rev. Lett. **89**, 093901 (2002).

[4] M. G. Silveirinha and C. Fernandes, IEEE Trans. Microw. Theory Tech. **53**, 1418 (2005).

[5] A. J. Hoffman, L. V. Alekseyev, S. S. Howard, K. J. Franz, D. Wasserman, V. A. Podolskiy, E. E. Narimanov, D. L. Sivco, and C. Gmachl, Nat. Mater. **6**, 946 (2007).

[6] C. R. Simovski, P. A. Belov, A. V. Atrashchenko, and Y. S. Kivshar, Adv. Mater. **24**, 4229 (2012).

[7] K. L. Koshelev and A. A. Bogdanov, Phys. Rev. B **92**, 085305 (2015).

[8] A. A. Bogdanov and R. A. Suris, Phys. Rev. B **83**, 125316 (2011).

[9] A. V. Chebykin, A. A. Orlov, A. V. Vozianova, S. I. Maslovski, Y. S. Kivshar, and P. A. Belov, Phys. Rev. B **84**, 115438 (2011).

[10] M. G. Silveirinha, J. Baena, L. Jelinek, and R. Marqués, Metamaterials **3**, 115 (2009).

[11] R.-L. Chern, Opt. Express **21**, 16514 (2013).

[12] M. G. Silveirinha, Phys. Rev. B **79**, 035118 (2009).

[13] A. A. Bogdanov and R. A. Suris, JETP Lett. **96**, 49 (2012).

[14] V. L. Ginzburg, *The Propagation of Electromagnetic Waves in Plasmas*, International Series of Monographs in Electromagnetic Waves, 2nd ed. (Pergamon, Oxford, 1970).

[15] A. V. Chebykin, M. A. Gorlach, and P. A. Belov, Phys. Rev. B **92**, 045127 (2015).

[16] S. I. Pekar, J. Phys. Chem. Solids **5**, 11 (1958).

[17] J. Stiebling and H. Raether, Phys. Rev. Lett. **40**, 1293 (1978).

[18] P. A. Belov, R. Marqués, S. I. Maslovski, I. S. Nefedov, M. G. Silveirinha, C. R. Simovski, and S. A. Tretyakov, Phys. Rev. B **67**, 113103 (2003).

[19] A. A. Orlov, S. V. Zhukovsky, I. V. Iorsh, and P. A. Belov, Photon. Nanostruct. Fund. Applic. **12**, 213 (2014).

[20] O. Schnitzer, V. Giannini, R. V. Craster, and S. A. Maier, Phys. Rev. B **93**, 041409 (2016).

[21] A. A. Orlov, P. M. Voroshilov, P. A. Belov, and Y. S. Kivshar, Phys. Rev. B **84**, 045424 (2011).

[22] J. Elser, V. A. Podolskiy, I. Salakhutdinov, and I. Avrutsky, Appl. Phys. Lett. **90**, 191109 (2007).

[23] G. A. Wurtz, R. Pollard, W. Hendren, G. Wiederrecht, D. Gosztola, V. Podolskiy, and A. V. Zayats, Nat. Nanotechnol. **6**, 107 (2011).

[24] S. Ishii and E. Narimanov, Sci. Rep. **5**, 17824 (2015).

[25] W. Yan, N. A. Mortensen, and M. Wubs, Opt. Express **21**, 15026 (2013).

[26] Under the term *longitudinal mode*, we understand the mode for which wave vector **k** is collinear to the electric field **E**.

[27] L. Tonks and I. Langmuir, Phys. Rev. **33**, 195 (1929).

[28] Y. Shimotsuma, P. G. Kazansky, J. Qiu, and K. Hirao, Phys. Rev. Lett. **91**, 247405 (2003).

[29] S. T. Ivanov and N. I. Nikolaev, J. Phys. D Appl. Phys. **32**, 430 (1999).

[30] C. R. Doerr and H. Kogelnik, J. Lightwave Technol. **26**, 1176 (2008).

[31] R. E. Collin, *Field Theory of Guided Waves* (IEEE Press, New York, 1991).

[32] W. L. Barnes, A. Dereux, and T. W. Ebbesen, Nature (London) **424**, 824 (2003).

[33] J. M. Pitarke, V. M. Silkin, E. V. Chulkov, and P. M. Echenique, Rep. Prog. Phys. **70**, 1 (2007).

[34] J. Polo and A. Lakhtakia, Laser Photon. Rev. **5**, 234 (2011).

[35] J. D. Jackson, Opt. Encyclopedia (2007), doi: 10.1002/9783527600441.oe014.

[36] A. Poddubny, I. Iorsh, P. Belov, and Y. Kivshar, Nat. Photon. **7**, 948 (2013).

[37] L. Ferrari, C. Wu, D. Lepage, X. Zhang, and Z. Liu, Prog. Quantum Electron. **40**, 1 (2015).

[38] M. Leontovich, Sov. Phys. JETP **13**, 634 (1961).

[39] F. Sauter, Z. Phys. **203**, 488 (1967).

[40] V. M. Agranovich and V. Ginzburg, *Crystal Optics with Spatial Dispersion and Excitons* (Springer, Berlin, 1984).

[41] A. A. Rukhadze and V. P. Silin, Sov. Phys. Usp. **4**, 459 (1961).

[42] V. M. Agranovich and V. I. Yudson, Opt. Commun. **7**, 121 (1973).

[43] F. Forstmann, Z. Phys. B Con. Mat. **32**, 385 (1979).

[44] F. Forstmann and R. R. Gerhardts, in *Advances in Solid State Physics*, Vol. 109 (Springer, Berlin, 1986), p. 291.

[45] W. Davis and C. Krowne, IEEE Trans. Antenn. Propag. **36**, 97 (1988).

[46] S. Scandolo, F. Bassani, and V. Lucarini, Eur. Phys. J. B **23**, 319 (2001).

[47] G. Barton, Rep. Prog. Phys. **42**, 963 (1979).

[48] A. D. Boardman, in *Electromagnetic Surface Modes*, edited by A. D. Boardman (Wiley, New York, 1982).

[49] N. A. Mortensen, Photon. Nanostruct. **11**, 303 (2013).

[50] G. Toscano, S. Raza, A.-P. Juaho, N. A. Mortensen, and M. Wubs, Opt. Express **20**, 4176 (2012).

[51] T. Christensen, W. Yan, S. Raza, A.-P. Jauho, N. A. Mortensen, and M. Wubs, ACS Nano **8**, 1745 (2014).

[52] S. Raza, S. I. Bozhevolnyi, M. Wubs, and N. A. Mortensen, J. Phys.: Condens. Matter **27**, 183204 (2015).

[53] S. I. Maslovski and S. A. Tretyakov, in *Proceedings of 8th International Conference on Electromagnetics of Complex Media* (http://www.lx.it.pt/Bian2000/Bian'00_files/Bian'00Prog_files/maslov1.ps, 2000).

[54] W. Yan, M. Wubs, and N. A. Mortensen, Phys. Rev. B **86**, 205429 (2012).

[55] Y. Tyshetskiy, S. V. Vladimirov, A. E. Ageyskiy, I. I. Iorsh, A. Orlov, and P. A. Belov, J. Opt. Soc. Am. B **31**, 1753 (2014).

[56] See Supplemental Material at http://link.aps.org/supplemental/10.1103/PhysRevB.94.115439 for the technical details about the derivation of dispersion equation taking into account the additional boundary condition and the numerical solution of complex dispersion equations in the presence of losses.

[57] H. Kogelnik and C. Shank, J. Appl. Phys. **43**, 2327 (1972).

[58] R. F. Kazarinov and R. A. Suris, Sov. Phys. Semicond. USSR **6**, 1184 (1973).

[59] V. M. Agranovich, *Surface Polaritons*, Vol. 1 (Elsevier, North Holland, 2012).

[60] S. A. Maier and H. A. Atwater, J. Appl. Phys. **98**, 011101 (2005).

[61] S. Raza, T. Christensen, M. Wubs, S. I. Bozhevolnyi, and N. A. Mortensen, Phys. Rev. B **88**, 115401 (2013).

[62] R. H. Renard, J. Opt. Soc. Am. **54**, 1190 (1964).

[63] A. Snyder and J. Love, Appl. Opt. **15**, 236 (1976).

[64] M. Mcguirk and C. K. Carniglia, J. Opt. Soc. Am. **67**, 103 (1977).

[65] W. J. Wild and C. L. Giles, Phys. Rev. A **25**, 2099 (1982).
[66] G. M. Gehring, A. C. Liapis, S. G. Lukishova, and R. W. Boyd, Phys. Rev. Lett. **111**, 030404 (2013).
[67] K. L. Tsakmakidis, A. D. Boardman, and O. Hess, Nature (London) **450**, 397 (2007).
[68] M. J. Adams, *An Introduction to Optical Waveguides* (Wiley, Chichester, 1981).
[69] J. A. Dionne, L. A. Sweatlock, H. A. Atwater, and A. Polman, Phys. Rev. B **72**, 075405 (2005).
[70] A. Bogdanov and R. Suris, Phys. Status Solidi B **249**, 885 (2012).
[71] P. Yao, C. Van Vlack, A. Reza, M. Patterson, M. M. Dignam, and S. Hughes, Phys. Rev. B **80**, 195106 (2009).
[72] K. L. Tsakmakidis, T. W. Pickering, J. M. Hamm, A. F. Page, and O. Hess, Phys. Rev. Lett. **112**, 167401 (2014).
[73] A. Reza, M. Dignam, and S. Hughes, Nature (London) **455**, E10 (2008).
[74] J. G. Pedersen, S. Xiao, and N. A. Mortensen, Phys. Rev. B **78**, 153101 (2008).
[75] K. L. Tsakmakidis, X. Zhang, and O. Hess, Proc. SPIE **9162**, 91621Y (2014).